

On the Estimation of the Mission Performance Index of Unmanned Surface Vehicles Based on the Mission Coverage Area

Jae-Yong Lee, Nam-Sun Son*

Department of Autonomous & Intelligent Maritime Systems Research Division,
Korea Research Institute of Ships & Ocean Engineering, Daejeon, Korea

Received November 12, 2021; received in revised form 07 May 2022; accepted 08 May 2022

DOI: <https://doi.org/10.46604/aiti.2023.10548>

Abstract

For mission planning and replanning of multiple unmanned surface vehicles (USVs), it is important to estimate each USV's mission performance in terms of sea surveillance (e.g., illegal ship control). In this study, a mission performance index (MPI) is proposed based on the mission coverage area for estimating the USVs' mission performance of illegal ship control. The penalty value is considered in the MPI calculation procedure owing to the track-off of the USV. In addition, the USV simulation is conducted under illegal ship control, and the MPI is calculated based on changing the mission coverage area. The results show that the MPI increases with the path width of the mission coverage area.

Keywords: unmanned surface vehicle (USV), mission coverage area, mission performance index (MPI), illegal ship control, USV simulation

1. Introduction

Generally, an unmanned surface vehicle (USV) is a small ship (1.5 to 15 m and 0.5 to 9 t) that can be controlled remotely or autonomously to perform missions under unfavorable weather conditions [1]. Although USVs are typically developed for military use, they have also been applied to marine transportation, marine surveys, response to trespassing ships in sea farms, sea rescue, and fusion with underwater remotely operated vehicles [2-5]. Furthermore, the International Maritime Organization has been reviewing international agreements on maritime safety and security regarding maritime autonomous surface ships [6].

Currently, Asian countries (e.g., Korea) are conducting government-supported projects in maritime industries, such as shipping, ports, shipbuilding, and offshore [7]. Recently, owing to the Fourth Industrial Revolution, unmanned, automated, and online fields have been highlighted. Accordingly, USV-related studies have been conducted to support or replace the missions performed by manned ships [8-9].

In particular, illegal ship control is important for monitoring USVs for mission planning and replanning [10]. In this study, the mission performance index (MPI) is defined to estimate the mission performance of multiple USVs using the mission coverage area for sea surveillance, such as illegal ship control. The MPI is estimated using the resulting trajectory of the USV, which is the ratio of the individual mission area to the total mission coverage area. To evaluate the MPI, a USV simulation is conducted under illegal ship control. In this study, the features of the MPI for the USV and the simulation results are described.

* Corresponding author. E-mail address: nso@kriso.re.kr

Tel.: +82-42-3636; Fax: +82-42-3624

Previous studies pertaining to path following and target tracking are explained in Section 2. The proposed MPI-based estimation method for USVs is presented in Section 3. The verification of the MPI via simulation is described in Section 4, and the conclusions and future studies are provided in Section 5.

2. Previous Path-Following and Target-Tracking Investigations

In the Korea Research Institute of Ships and Ocean Engineering, the Aragon series of USVs (Aragon1, Aragon2, and Aragon3) was developed through a project entitled “Development of Multipurpose Intelligent Unmanned Surface Vehicle” [10]. Recently, USV swarms have been investigated using the Aragon series of USVs through a project entitled “Development of Situation Awareness and Autonomous Navigation Technology of USV Based on Artificial Intelligence” [11].

In this study, a USV (Aragon1) was used as an illegal ship to simulate illegal ship control, where the vehicle steers away from a patrol ship (i.e., another USV (Aragon3)) via path following. Therefore, a path-following algorithm is required when Aragon3 trails Aragon1’s escape path. Previously, a path-following algorithm was developed using the line-of-sight (LOS) [12]. As shown in Fig. 1, the heading angle must be controlled for path-following control. In this case, WP_k is the waypoint of k (X_k, Y_k), P_t is the current position (X_t, Y_t) of the USV, Ψ_t is the heading angle, and δ_t is the nozzle angle of the waterjet. The target heading angle (Ψ_{tc}) was calculated using the waypoint of k , and the position of Aragon1 was calculated using the LOS for path following [12].

In other words, Aragon3 was used for illegal ship control. A target-tracking algorithm is required for a patrol ship (i.e., Aragon3). Yun et al. [13] developed a target-tracking algorithm using the concept of virtual points, as illustrated in Fig. 2. Their proposed USV was used as a patrol ship to track the target ship (illegal ship) in the starboard and port or stern. When tracking a target ship, the USV must maintain a certain direction with a separation distance at a specific speed. As shown in Fig. 2, the USV tracks the target ship via virtual points “A” and “B.” In this case, virtual point “A” is generated by the heading angle of the target ship, and virtual point “B” is generated by the separation distance from the target ship. The target-tracking algorithm is based on tracking a target ship with the LOS angle.

In addition, various international studies related to path following and target tracking have been conducted [14]. An improved LOS guidance algorithm that can be adjusted based on the path-following error was investigated [15]. Additionally, a deep reinforcement learning method for solving the path-following problem of the USV has been investigated based on the decision-making network [16-17]. The straight-line target control of USVs has been investigated based on maneuverability and agility using the straight-line concept with high speed [18].

The purpose of this study is to estimate the MPI using the resulting trajectory of an illegal ship (Aragon1) and a patrol ship (Aragon 3). In this study, the path-following algorithm is applied to an illegal ship (Aragon1) using the LOS, and the target-tracking algorithm is applied to the patrol ship (Aragon3) using the concept of virtual points.

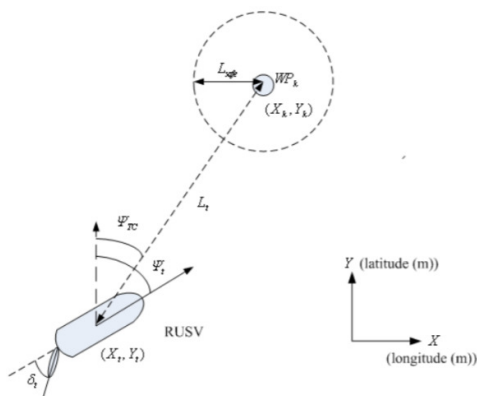


Fig. 1 Path-following algorithm [12]

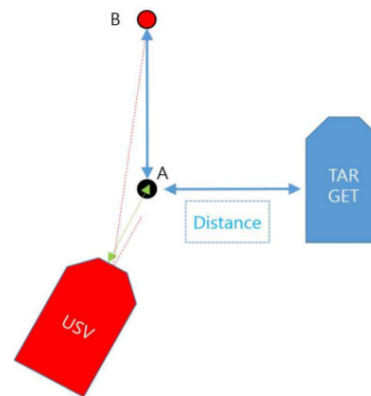


Fig. 2 Target-tracking algorithm [13]

3. Estimation of MPI

3.1. Concept of MPI

The performance of USVs for mission planning and replanning is to be estimated. The MPI is calculated using the resulting trajectory of the USV, i.e., the ratio of the individual mission area to the mission coverage area. As shown in Fig. 3, the mission coverage area is in the sea environment of illegal ship control, where the fairways of ships are extremely narrow owing to fish farms, tides, and reefs. The MPI is to be analyzed while the path width of the mission coverage area is changed from “2L” to “6L.” In addition, if the USV is outside the mission coverage area, then MPI* is applied to estimate the MPI while considering the penalty, as shown in Fig. 4.

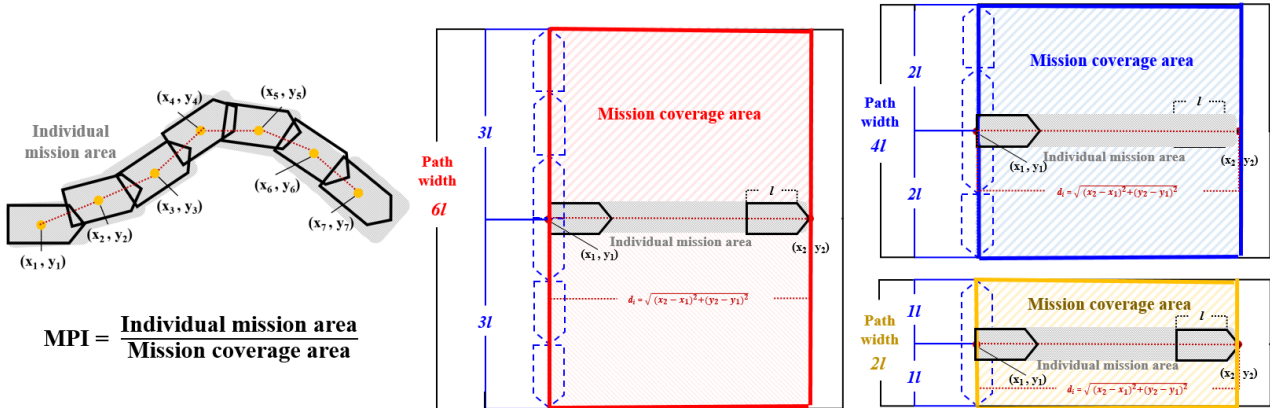


Fig. 3 Concept of MPI and cases of mission coverage area with various path widths

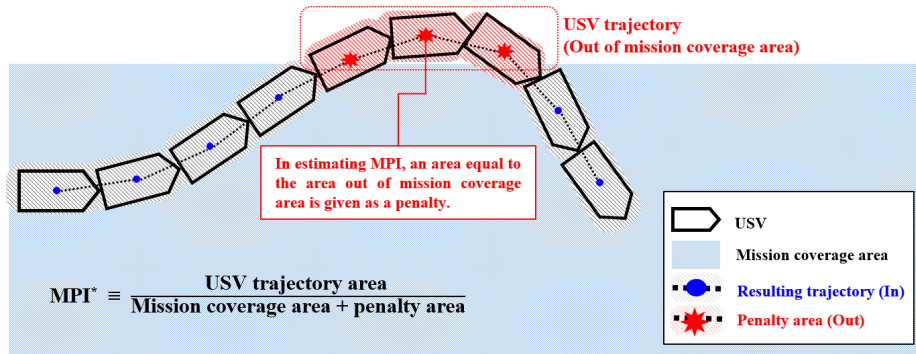


Fig. 4 Concept of MPI and penalty area

3.2. Procedure of MPI estimation

In this study, the MPI was estimated to analyze the mission performance of the USVs. The overall procedure is summarized in Table 1. First, the USV information was input, including the name, length, breadth, and speed of the USV. The trajectory information of the USV was selected from the simulation results, and the mission coverage area was set using various path widths. Next, the penalty area was calculated by considering the track-off from the mission coverage area. Finally, the MPI was estimated using the mission coverage area and penalty area.

Table 1 Procedure for estimating MPI*

Step	Description
1	Input information of USV
2	Select trajectory information of USV
3	Set mission coverage area (path width: 2L to 6L) of USV
4	Calculate USV trajectory area
6	Calculate penalty area
7	Estimate MPI

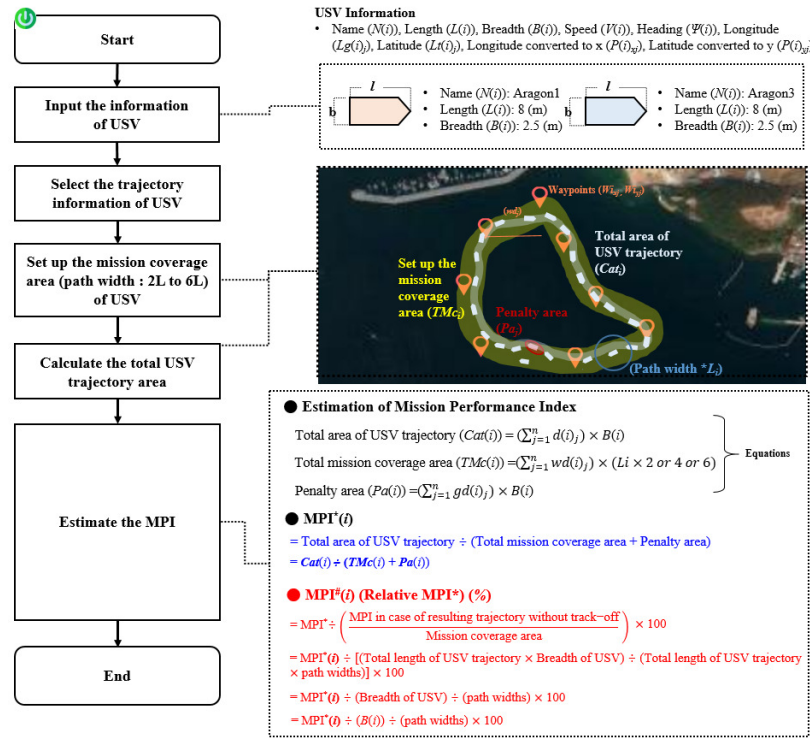


Fig. 5 Flowchart for estimating MPI

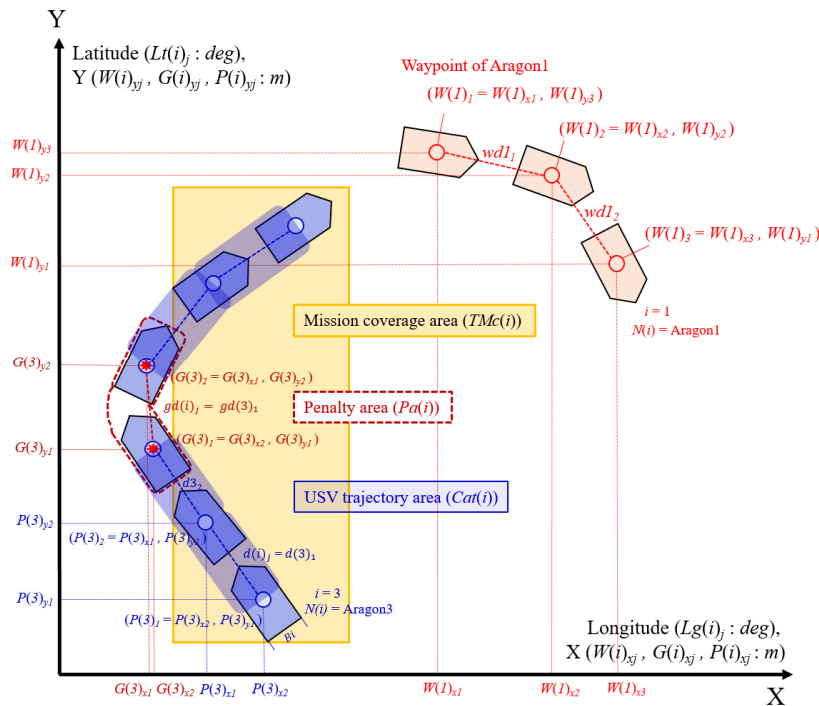


Fig. 6 Example of MPI estimation

A flowchart of MPI estimation is shown in Fig. 5. The path width was changed from 2L to 6L to verify the change in the estimated MPI. Furthermore, the total area of the USV trajectory ($Cat(i)$), total mission coverage area ($TMc(i)$), and penalty area ($Pa(i)$) were calculated using the equations shown in Fig. 5. $MPI\#(i)$ is the ratio of the relative $MPI\#(i)$ of the USV to the MPI in the case of the resulting trajectory without track-off.

An example of MPI estimation is shown in Fig. 6. The notations used in MPI estimation are presented in the nomenclature section. Here, information regarding Aragon1 and Aragon3 is shown, such as the latitude, longitude, waypoints, speed, and heading. The mission coverage area (Eq. (1)), USV trajectory area (Eq. (2)), and penalty areas (Eq. (3)) are calculated as follows:

$$TMc(i) = (\sum_{j=1}^n wd(i)_j) \times (Li \times 2 \text{ or } 4 \text{ or } 6) \tag{1}$$

$$Cat(i) = (\sum_{j=1}^n d(i)_j) \times B(i) \tag{2}$$

$$Pa(i) = (\sum_{j=1}^n gd(i)_j) \times B(i) \tag{3}$$

4. Simulation and Results

4.1. Simulation scenario

In this study, a simulation pertaining to the illegal control of a USV was conducted in Gwangam Port, Korea to verify the proposed MPI-based estimation method. As illegal ships frequently appear on sea farms, a sea farm was selected as the game area for the simulation. Aragon1 was used as an illegal ship, and Aragon3 was used as a patrol ship for illegal ship control. The escape path of Aragon1 was planned in advance by considering the zone of the sea farm, as shown in Fig. 7, and Aragon1 trailed this path using the path-following algorithm based on the LOS [12]. Aragon3 chased the illegal ship (Aragon1) for illegal ship control using the target control algorithm based on the concept of virtual points [13].

Table 2 summarizes the information regarding Aragon1 and Aragon3. The USV simulation was conducted via dynamic simulation based on the Nomoto model [19]. The resulting trajectories of Aragon1 and Aragon3 using the path-following and target-tracking algorithms are shown in Fig. 8. Fig. 9 shows the histories of the speed and heading angle of Aragon1 and Aragon3 based on the simulation.

As shown in Figs. 8 and 9, the simulation was conducted with the path widths ranging from “2L” to “6L” to verify the change in the estimated MPI. The red and blue lines represent the resulting trajectories of Aragon1 and Aragon3, respectively. The path-following algorithm of Aragon1 was successfully conducted at a speed of 10 knots. Furthermore, the target control algorithm of Aragon3 was successfully implemented at a high speed in the simulation. The heading error between Aragon1 and Aragon3 can be determined because Aragon3 tracks Aragon1 via the target-tracking algorithm on the stern side.



Fig. 7 Path of Aragon1 and location of sea farm

Table 2 Information regarding Aragon1 and Aragon3

No.	Ship	Length (m)	Breadth (m)	Maximum speed (knot)
1	Illegal ship (Aragon1)	8	2.5	10
2	Patrol ship (Aragon3)	8	2.5	max 20

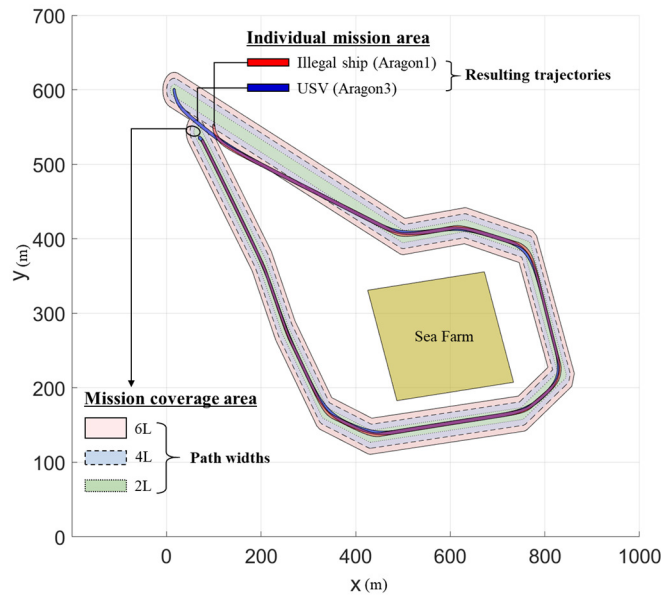
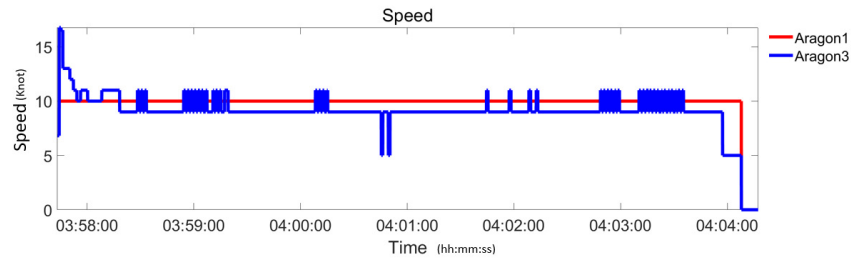
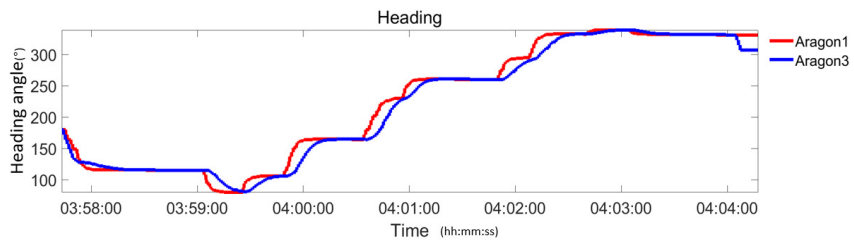


Fig. 8 Resulting trajectories of Aragon1 and Aragon3



(a) Speed of Aragon1 and Aragon3



(b) Heading angle of Aragon1 and Aragon3

Fig. 9 Time histories of the speed and heading angle of Aragon1 and Aragon3

4.2. Analysis of MPI based on simulation results

As shown in Tables 3 and 4, the MPI* exceeds 95% for the illegal ship (Aragon1) and patrol ship (Aragon3). This implies that Aragon1 successfully conducted path following as an illegal ship, and Aragon3 successfully conducted target tracking as a patrol ship. The MPI# of Aragon1 was 4.9% higher than that of Aragon3, on average. This is because Aragon1 adhered to the designated path, whereas Aragon3 tracked Aragon1. Therefore, Aragon3 exhibited track-off in target control owing to the heading error during target tracking. Furthermore, as the path width of the mission coverage area widened (from 2L to 6L), MPI# increased because the penalty area in both Aragon1 and Aragon3 reduced.

Table 3 MPI results

Mission coverage area	Index	Units	Aragon1	Aragon3
2L	Cat(i)	(m ²)	4,611.62	4,847.85
	Np(i)	(ea)	84	1,399
	Pa(i)	(m ²)	210	3,497.5
	TMc(i)	(m ²)	29,948.91	31,591.37

Table 3 MPI results (continued)

Mission coverage area	Index	Units	Aragon1	Aragon3
4L	Cat(i)	(m ²)	4,611.62	4,847.85
	Np(i)	(ea)	25	858
	Pa(i)	(m ²)	62.5	2,145
	TMc(i)	(m ²)	60,084.80	63,563.23
6L	Cat(i)	(m ²)	4611.62	4,847.85
	Np(i)	(ea)	0	299
	Pa(i)	(m ²)	0	747.5
	TMc(i)	(m ²)	89,869.70	95,389.62

Table 4 Comparative analysis of relative MPI* without track-off

Path width	USV	MPI*	MPI# (%)
		= $Cat(i) \div (TMc(i) + Pa(i))$	= $MPI^* \div [(B(i)) \div (\text{path widths})] \times 100$
2L	Aragon1	0.1529	97.86
	Aragon3	0.1381	88.42
4L	Aragon1	0.0766	98.14
	Aragon3	0.0738	94.44
6L	Aragon1	0.0513	98.52
	Aragon3	0.0504	96.82

5. Conclusions and Future Studies

In this study, an MPI was defined to estimate the mission performance of multiple USVs using the mission coverage area. In particular, the penalty value was considered in the MPI calculation procedure owing to the track-off of the USV. To verify the proposed MPI-based estimation method, illegal ship control was simulated using an illegal ship (Aragon1) and a patrol ship (Aragon3). The illegal ship (Aragon1) and patrol ship (Aragon3) successfully conducted path following and target tracking, respectively. Therefore, the MPI exceeded 4.9%. The MPI of the illegal ship (Aragon1) was higher than that of the patrol USV (Aragon3) because Aragon1 adhered to the designated path, whereas Aragon3 indicated track-off during target tracking. Furthermore, as the path width of the mission coverage area increased (from 2L to 6L), the MPI increased owing to a decrease in the penalty area. In the future, the authors will conduct an experiment pertaining to illegal ship control in an actual sea using multiple USVs; subsequently, the experimentally obtained MPI will be compared with simulation results.

Nomenclature

Notation	Units	Definition
i	-	Number of <i>i</i> th USVs (Aragon1 or Aragon3)
N(i)	-	Name of <i>i</i> th USV (Aragon1 or Aragon3)
L(i)	m	Length of <i>i</i> th USV
B(i)	m	Breadth of <i>i</i> th USV
V(i)	knot	Speed of <i>i</i> th USV
Ψ(i)	°	Heading of <i>i</i> th USV
Lg(i) _j	°	<i>j</i> th trajectory point of longitude for <i>i</i> th USV
Lt(i) _j	°	<i>j</i> th trajectory point of latitude for <i>i</i> th USV
P(i) _{xj}	m	X value converted from <i>Lg</i> _{<i>j</i>} of <i>j</i> th trajectory point in <i>i</i> th USV
P(i) _{yj}	m	Y value converted from <i>Lt</i> _{<i>j</i>} of <i>j</i> th trajectory point in <i>i</i> th USV
d(i) _j	m	Distance between USV trajectories; $d(i)_j = \sqrt{(P(i)_{xn} - P(i)_{xn-1})^2 + (P(i)_{yn} - P(i)_{yn-1})^2}$
Td(i) _j	m	Total distance of USV trajectory; $Td(i)_j = \sum_{j=1}^n d(i)_j$
Cat(i)	m ²	Total USV trajectory area; $Cat(i) = Td(i)_j \times B(i)$
W(i) _{xj}	m	X of <i>j</i> th waypoint for <i>i</i> th USV
W(i) _{yj}	m	Y of <i>j</i> th waypoint for <i>i</i> th USV

$wd(i)_j$	m	Distance between waypoints; $wd(i)_j = \sqrt{(W(i)_{xn} - W(i)_{xn-1})^2 + (W(i)_{yn} - W(i)_{yn-1})^2}$
$TMc(i)$	m^2	Total mission coverage area; $TMc(i) = \sum_{j=1}^n (wd(i)_j \times (L(i) \times \text{path width}))$
$G(i)_{xj}$	m	X of j^{th} waypoint for i^{th} USV outside mission coverage area
$G(i)_{yj}$	m	Y of j^{th} waypoint for i^{th} USV outside mission coverage area
$gd(i)_j$	m	Distance between waypoints outside mission coverage area; $\sqrt{(P(i)_{xn} - G(i)_{xn})^2 + (P(i)_{yn} - G(i)_{yn})^2}$
$Np(i)$	-	Number of points deviating from mission coverage area for i^{th} USV (ea)
$Pa(i)$	m^2	Penalty area; $Pa(i) = \sum_{j=1}^n (gd(i)_j) \times B(i)$
$MPI(i)$	-	Mission performance index; $MPI(i) = Cat(i) \div (TMC + Pa(i))$
$MPI^{\#}(i)$	%	Ratio of relative MPI^* of USV to MPI for case involving resulting trajectory without track-off; $MPI^{\#}(i) = MPI^* \div (B(i)) \div (\text{path width}) \times 100$

Acknowledgments

This study was supported by the project titled “Development of Situation Awareness and Autonomous Navigation Technology of Unmanned Surface Vehicle Based on Artificial Intelligence (PES3880, PES4270),” which was funded by the Korea Research Institute of Ships and Ocean Engineering.

Conflicts of Interest

The authors declare no conflicts of interest regarding the publication of this study.

References

- [1] V. Bertram, “Unmanned Surface Vehicles—A Survey,” Skibsteknisk Selskab, vol. 1, pp. 1-14, January 2008.
- [2] J. E. Manley, “Unmanned Surface Vehicles, 15 Years of Development,” Oceans, pp. 1-4, September 2008.
- [3] D. W. Jung, et al., “A Study on Unmanned Surface Vehicle Combined with Remotely Operated Vehicle System,” Proceedings of Engineering and Technology Innovation, vol. 9, pp. 17-24, July 2018.
- [4] J. Ansary, et al., “Swarms of Aquatic Unmanned Surface Vehicles (USV), a Review from Simulation to Field Implementation,” Proceedings of International Design Engineering Technical Conferences and Computers and Information in Engineering Conference, vol. 83914, pp. 436-528, August 2020.
- [5] N. S. Son, et al., “On the Sea Trial Test for the Validation of an Autonomous Collision Avoidance System of Unmanned Surface Vehicle, ARAGON,” Proceedings of the OCEANS 2018 MTS/IEEE Charleston, pp. 1-5, October 2018.
- [6] C. J. Chae, et al., “A Study on Identification of Development Status of MASS Technologies and Directions of Improvement,” Applied Sciences, vol. 10, no. 13, Article no. 4564, July 2020.
- [7] B. S. Hwang, et al., “The Fourth Industrial Revolution and Future Innovation: Policy Fields,” Proceedings of the Korea Technology Innovation Society Conference, pp. 436-528, August 2017.
- [8] R. Murphy, et al., “An Analysis of International Use of Robots for COVID-19,” Robotics and Autonomous Systems, vol. 148, Article no. 103922, February 2021.
- [9] S. Y. Kim, “Research Trends of USV,” Journal of the Society of Naval Architects of Korea, vol. 51, no. 2, p. 2, June 2014.
- [10] S. Y. Kim, et al., “Project: Development of Multi-Purpose Intelligent Unmanned Surface Vehicle,” Korea Institute of Ocean Science and Technology, Final Report PJT20040, August 15, 2019.
- [11] N. S. Son, “Project: Development of Situation Awareness and Navigation Technology of Unmanned Surface Vehicle Based on the Artificial Intelligence,” Korea Research Institute of Ships and Ocean Engineering, Report PES3880, January 2022.
- [12] N. S. Son, et al., “Study on a Waypoint Tracking Algorithm for Unmanned Surface Vehicle (USV),” Journal of Navigation and Port Research, vol. 33, no. 1, pp. 35-41, March 2009.
- [13] K. H. Yun, et al., “A Study on the Algorithm of Target Tracking System for USV Based on Simulation Method,” Journal of Ships and Ocean Engineering, vol. 56, pp. 19-25, December 2015.
- [14] M. A. bin Mansor, et al., “Motion Control Algorithm for Path Following and Trajectory Tracking for Unmanned Surface Vehicle: A Review Paper,” Proceedings of the 3rd International Conference on Control, Robotics, and Cybernetics, pp. 73-77, September 2018.

- [15] T. Liu, et al., "Path Following Control of the Underactuated USV Based on the Improved Line-of-Sight Guidance Algorithm," *Journal of Polish Maritime Research*, vol. 24, no. 1, pp. 3-11, April 2017.
- [16] Y. Zhao, et al., "Path Following Optimization for an Underactuated USV Using Smoothly-Convergent Deep Reinforcement Learning," *IEEE Transactions on Intelligent Transportation Systems*, vol. 22, no. 10, pp. 6208-6220, October 2021.
- [17] J. H. Woo, et al., "Deep Reinforcement Learning-Based Controller for Path Following of an Unmanned Surface Vehicle," *Ocean Engineering*, vol. 183, pp. 155-166, July 2019.
- [18] M. Breivik, et al., "Straight-Line Target Tracking for Unmanned Surface Vehicles," *Modeling, Identification, and Control*, vol. 29, no. 4, pp. 131-149, April 2008.
- [19] T. I. Fossen, *Guidance and Control of Ocean Vehicles*, New York: John Wiley and Sons, 1994.



Copyright© by the authors. Licensee TAETI, Taiwan. This article is an open access article distributed under the terms and conditions of the Creative Commons Attribution (CC BY-NC) license (<https://creativecommons.org/licenses/by-nc/4.0/>).